International Journal of Engineering Research & Technology (IJERT)
ISSN: 2278-0181
Vol. 3 Issue 8, August - 2014

Effects of MHD Laminar Flow Between a Fixed Impermeable Disk and a Porous Rotating Disk

Hemant Poonia*
* Asstt. Prof., Deptt. of Math, Stat & Physics,
CCSHAU, Hisar-125004.

R. C. Chaudhary†
† Retd. Professor, Deptt. of Maths,
Univ. of Rajasthan, Jaipur-302022.

Abstract: We formulate a mathematical model that governs operations of many engineering systems particularly the Ceiling fan to explain the fluid flow between the fixed impermeable and the porous rotating disks in the presence of a transverse magnetic field. The model is based on the continuity and the Navier-stokes equations which are reduced into set of coupled ordinary differential equations through transformation by similarity variables. The coupled ordinary differential equations are solved using perturbation techniques. The results for the velocity profiles and the fluid pressure distribution are displayed graphically showing the effects of various parameters. The graphical results of the shear stress are presented and discussed.

Keywords: Impermeable disk, Porous rotating disk, Incompressible viscous fluid, Shear flows, MHD.
MSC2010: 76D03, 76D05, 76F10, 76U05, 76W05.

INTRODUCTION

The problem of laminar flow between two parallel disks stemming from both practical interests (e. g. ocean circulation motion and turbo machinery applications) and theoretical interests (e. g. exact solutions of the Navier-stokes equations in certain geometric limiting cases) has received much attention over the years. In modern times, the theory of flow through convergent- divergent channels has many applications in aerospace, chemical, civil, environmental, mechanical and bio-mechanical engineering as well as in understanding rivers and canals. Due to the complexity of a real fluid flow, certain assumptions are made to simplify the mathematical convenience. Some of the basic assumptions are, the fluid is ideal (i.e. without viscosity for mathematical convenience). In situations where the effect of viscosity is small, this assumption often yields results of acceptable accuracy although where viscosity plays a major part (e. g. in boundary layers), the assumption is clearly untenable. The flow is steady (i.e. the flow parameters do not change with time). The fluid is incompressible.

We consider the flow between a fixed impermeable disk and a porous rotating disk (Fig.(a)) both being immersed in a large body of fluid. Motion of the fluid is induced by the rotation of the porous disk. This study is interesting in its own right and also based on its applicability.

In the sequel, the following notation will be used:

L= distance between the two disks.
r = Radius of each disk.
Ω= Angular speed of the rotating disk.
ε = Measure of the angular speed or momentum of the rotating porous disk.
W= Suction velocity at which fluid is withdrawn from the rotating disk (injection if W is Negative).
u, v, w = Velocity components in the directions r, ϕ and z respectively.

f, g, p are the similarity variables used to reduce the Navier-stokes non-linear partial differential equations into a system of non-linear ordinary differential equations. For fixed impermeable disk, u=0, w=0, v=0 while for porous rotating disk, u=0, w=W, v=rΩε. The disks are separated by a distance L which is small compared to their radii.

The direction of fluid flow as shown by the arrows in the figure (a) is heading towards the porous disk which is rotating with a constant angular speed Ω. The suction velocity is assumed to be constant and equal to W. The rotation speed is given by Ωε, where Ω is the angular speed of the rotating disk and the parameter ε is a regulator which controls rotation of the disk ($0 \le \varepsilon \le 1$). If $\varepsilon = 0$, then there is no rotation but for $\varepsilon > 0$, rotating occurs.

The question of existence and uniqueness of solutions in the similarity formulation has been raised [16]. Moreover, a question on the behavior of the flow between the two disks and in particular near the stationary disk as the speed of the

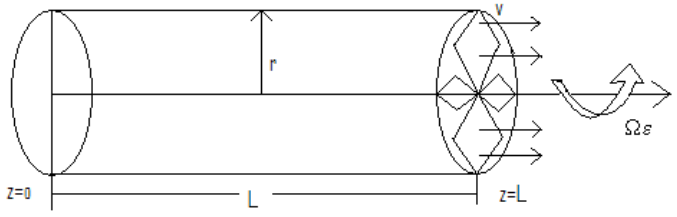

Fig.(a) Physical model representing laminar flow between parallel disks.

rotating disk approaches infinity has not been satisfactorily addressed in this type of formulation. The simplified equations that govern the flow over an infinite rotating disk, is studied by Kuiken [12] and Kelson et al. [10]. Theoretical work on this class of flows has been

undertaken mainly in the framework of similarity solutions because the assumption of self-similarity to reduce Navier-stokes equations from partial to ordinary differential equations greatly simplifies the analysis. Stuart [23] showed that the effect of suction is to thin the boundary layer by decreasing the radial and azimuthal components of the velocity while at the same time increasing the axial flow towards the disk at infinity. Turkyilmazoglu [24] extended the classical von-Karman problem of flow over a rotating disk to account for compressibility effects with insulated and isothermal wall conditions. He used an exponentially decaying series method to find the solution of the steady laminar flow of an incompressible, viscous, electrically-conducting fluid over a rotating disk in the presence of a uniform transverse magnetic field.

The study of the motion of a viscous incompressible rotating fluid is of considerable interest in recent years due to its wide applications in cosmical and geophysical fluid dynamics. The research papers dealing with rotating fluid have appeared, for example, Vidyanidhi and Nigam [26], Puri [20], Jana and Dutta [8]. In a recent paper, Mazumder [15] and in a note, Ganapathy [6] gave an approximate solution of the oscillatory couette flow between two infinite parallel plates in a rotating system under boundary layer approximations. Pearson [19], Lance and Rogers [13] obtained the numerical solution of this problem. Gaur [7] discussed the same problem by considering the effect of porosity. Khare [11] studied the problem of axisymmetric steady flow of a viscous incompressible fluid between two co-axial circular disks, one rotating and the other stationary with uniform suction at stationary disk for electrically conducting viscous fluid in the presence of a transverse magnetic field. Purohit and Patidar [21] studied the steady flow and heat transfer of a viscous incompressible fluid between two infinite rotating disks for small Reynolds number, where rate of suction of one disk is different from the rate of injection at the other disk. Recently Das and Aziz [4] extended the problem investigated by Purohit and Patider [21] including transverse magnetic field where rate of suction in one disk is different to that the rate of injection at other. Sibanda and Makinde [22] investigated the heat transfer characteristics of steady MHD flow in a viscous electrically conducting incompressible fluid with Hall current past a rotating disk with ohmic heating and viscous dissipation. They found that the magnetic field retards the fluid motion due to the opposing Lorentz force generated by the magnetic field. Turkyilmazoglu [24] concluded the exact solutions for the incompressible viscous magnetohydrodynamic fluid of a rotating disk flow.

The effects of an axial magnetic field applied to the fluid with Hall effects are studied by Attia and Aboul-Hassan [1]. Maleque and Sattar [14] have considered the effects of variable fluid properties on laminar boundary layers, namely the density ρ, the viscosity μ and the thermal conductivity to flow due to a porous rotating disk. The effect of temperature dependent viscosity on the flow and heat transfer along a uniformly heated impulsively rotating disk in a porous medium is discussed by Attia [2]. Osalusi and Sibanda [17] studied the effects of variable properties with magnetic effect. Barik et al [3] considered hall effects on unsteady MHD flow between two rotating disks with non-coincident parallel axes.

Osalusi [18] analyzed the combined effects of slip and thermal radiation to the MHD flow and thermal fields over a rotating single disk. The unsteady Couette flow between two infinite horizontal parallel plates in a rotating system under boundary layer approximation is studied by Das et al. [5]. Kavenuke et al. [9] considered the modeling laminar flow between a fixed impermeable disk and a porous rotating disk both being immersed in a large body of the fluid.

Model and Analysis: Fig.(a) depicts a system of porous rotating disk and a stationary disk both being immersed in a large fluid body. Fluid motion is set up by both rotation of the porous disk and suction (or injection) of the fluid itself.

We use the cylindrical polar coordinates (r, ϕ, z) and the corresponding velocity components by (u, v, w). However, the angle ϕ will not appear in our analysis because of rotational symmetry. The plane z = L rotates about the z-axis with constant angular velocity Ωε and the suction velocity is given by W.

In order to neglect the end effects, we assume that the gap L is very small compared to the radii of the disks that is, L<< r (0 <L<< r).

The equations governing the motion of an incompressible viscous fluid arise from conservation of mass principle and the momentum principle.

From the conservation of mass principle, we have

$$\frac{1}{r}\frac{\partial(ru)}{\partial r}+\frac{\partial w}{\partial z}=0 \quad (1)$$

From the momentum principle and ignoring gravity we have the Navier-stokes equations, one for each co-ordinate direction

$$u\frac{\partial u}{\partial r}+w\frac{\partial u}{\partial z}=-\frac{1}{\rho}\frac{\partial P}{\partial r}+\upsilon\left[\frac{\partial^2 u}{\partial r^2}+\frac{\partial}{\partial r}\left(\frac{u}{r}\right)+\frac{\partial^2 u}{\partial z^2}\right]-\frac{\sigma B_0^2 u}{\rho}+\frac{v^2}{r} \quad (2)$$

$$u\frac{\partial v}{\partial r}+w\frac{\partial v}{\partial z}=\upsilon\left[\frac{\partial^2 v}{\partial r^2}+\frac{\partial}{\partial r}\left(\frac{v}{r}\right)+\frac{\partial^2 v}{\partial z^2}\right]-\frac{\sigma B_0^2 v}{\rho}-\frac{uv}{r} \quad (3)$$

$$u\frac{\partial w}{\partial r}+w\frac{\partial w}{\partial z}=\upsilon\left[\frac{\partial^2 w}{\partial r^2}+\frac{1}{r}\frac{\partial w}{\partial r}+\frac{\partial^2 w}{\partial z^2}\right]-\frac{1}{\rho}\frac{\partial P}{\partial z} \quad (4)$$

The small gap L between the two disks allows us to neglect the behavior of the flow around the edges. Therefore the bounding conditions to be specified are those applicable to velocity components at both disk surfaces and not the edges.

For the velocity, it is assumed that the no slip condition applies at the surface of the disks.
The boundary conditions are

$$\left.\begin{array}{l} u(r,0)=v(r,0)=w(r,0)=0 \quad at\ z=0 \\ u(r,L)=0, v(r,L)=r\Omega\varepsilon, w(r,L)=W \quad at\ z=L \end{array}\right]$$

(5)

Since the fluid is incompressible, it is possible to define the stream function from the governing continuity equation in two dimensions. This enables us to solve the continuity equation (1) in the familiar way by setting,

$$u=\frac{1}{r}\frac{\partial\psi}{\partial z}, w=-\frac{1}{r}\frac{\partial\psi}{\partial r}$$

(6)

and by defining a dimensionless normal distance from the disk.

$$\eta=\frac{z}{L}=\frac{\Omega z}{W}$$

(7)

We assume a similarity transformation of the form

$$\psi(r,n)=r^2 f(\eta)W$$

(8)

Equations (6) and (8) yield the expression for the radial and tangential velocities

$$u=r\Omega f'(\eta), w=-2Wf(\eta)$$

(9)

For the axial velocity and pressure variables, we assume that,

$$v=r\Omega g(\eta), p=-\frac{1}{2}\rho r^2 A\Omega^2+\rho P(\eta)$$

(10)

The corresponding boundary conditions for the functions f and g are

$$\left.\begin{array}{l} f'(0)=0, f(0)=0, g(0)=0 \\ f'(1)=0, f(1)=-\frac{1}{2}, g(1)=\varepsilon \end{array}\right]$$

(11)

Substituting (9) and (10) into equations (2) to (4), we obtain

$$\left[f'(\eta)\right]^2-2f(\eta)f''(\eta)-g^2(\eta)=A+\frac{1}{R}f'''(\eta)-Mf'(\eta)$$

(12)

$$2\left[f'(\eta)g(\eta)-f(\eta)g'(\eta)\right]=\frac{1}{R}g''(\eta)-Mg(\eta)$$

(13)

$$P'(\eta)=-4W^2 f'(\eta)f(\eta)-\frac{2W\upsilon}{L}f''(\eta)$$

(14)

Where, the primes denote differentiation with respect to η. The parameter $R=\frac{W^2}{\Omega\upsilon}$ is the Reynolds number and A is an arbitrary constant, $M=\frac{\sigma B_0^2}{\rho\Omega}$ is magnetic parameter, σ is the electrical conductivity, B_0 is the magnetic induction and ρ is the density.

Differentiating equation (12) with respect to η

$$-2\left[f(\eta)f''(\eta)+g(\eta)g'(\eta)\right]=\frac{1}{R}f'''(\eta)-Mf''(\eta)$$

(15)

Equation (13) can be written as

$$2\left[f'(\eta)g(\eta)-f(\eta)g'(\eta)\right]=\frac{1}{R}g''(\eta)-Mg(\eta)$$

(16)

Our main focus is on solving the two coupled non-linear ordinary differential equations (15) and (16), subject to the boundary conditions

$$\left.\begin{array}{l} f'(0)=0, f(0)=0, g(0)=0 \\ f'(1)=0, f(1)=-\frac{1}{2}, g(1)=\varepsilon \end{array}\right]$$

(17)

Though the transformation has provided a set of ordinary differential equations, a closed form solution is still not possible. Consequently, we apply the perturbation technique. Treating R as a perturbation parameter, substituting the expansions into

$$\left.\begin{array}{l} f=f_0+Rf_1+R^2 f_2+..... \\ g=g_0+Rg_1+R^2 g_2+..... \end{array}\right]$$

(18)

equations (15) and (16) transforms the intractable original problem into a sequence of simple ones. By collecting terms of the same order, we have

$$f_0'''(\eta)=0$$

(19)

$$g''(\eta)=0$$

(20)

$$-2\left[f_0(\eta)f_0'''(\eta)+g_0(\eta)g_0'(\eta)\right]=f_1'''(\eta)-Mf_0'(\eta)$$

(21)

$$2\left[f_0'(\eta)g_0(\eta)-f_0(\eta)g_0'(\eta)\right]=g_1''(\eta)-Mg_0(\eta)$$

(22)

Subject to the boundary conditions

$$f_0'(0)=f_0(0)=g_0(0)=0,\ f_0'(1)=0,\ f_0(1)=-\frac{1}{2},\ g_0(1)=\varepsilon$$
$$f_1'(0)=f_1(0)=g_1(0)=0,\ f_1'(1)=f_1(1)=g_1(1)=0$$

(23)

The solution of (19) to (22) under the given boundary conditions yields the following

$$f_0(\eta)=\eta^3-\frac{3}{2}\eta^2$$

(24)

$$g_0(\eta)=\varepsilon\eta$$

(25)

$$f_1(\eta)=-\frac{\eta^7}{70}+\frac{\eta^6(M+6)}{120}-\frac{\eta^5(3M+2\varepsilon^2)}{120}+\frac{B_1\eta^3}{6}+\frac{B_2\eta^2}{2}$$

(26)

$$g_1(\eta)=\varepsilon\left[\frac{\eta^5}{5}-\frac{\eta^4}{4}+\frac{M\eta^3}{6}+\frac{3-10M}{60}\right]$$

(27)

Where, $B_1=\frac{3}{7}-\frac{M+6}{5}+\frac{3}{20}(3M+2\varepsilon^2)$,

$$B_2=-\frac{8}{70}+\frac{M+6}{20}-\frac{3M+2\varepsilon^2}{30}$$

Fluid pressure distribution:

Integrating equation (14) from 0 to n and applying the boundary conditions, we obtain

$$P(r,\eta)-P(r,0)=-2W^2\left[f^2(\eta)-f^2(0)\right]-\frac{2W\upsilon}{L}\left[f'(\eta)-f'(0)\right]$$

(28)

$$P^*=\frac{P(r,\eta)-P(r,0)}{-2W^2}=f^2(\eta)+\frac{1}{R}f'(\eta)$$

(29)

Shear stress:

The action of velocity in the fluid adjacent to the disks tends to set a tangential shear stress which opposes the rotation of the disk. The tangential stresses at the rotating porous disk are given by

$$\tau_{\phi z}=\mu\frac{\partial v}{\partial z}=\frac{\mu r\Omega^2}{W}g'(1)$$

(30)

$$\tau_{\phi z}=\frac{\mu r\Omega^2\varepsilon}{W}\left(1+\frac{RM}{2}\right)$$

(31)

$$\tau_{zr}=\mu\frac{\partial u}{\partial z}=\frac{\mu r\Omega^2}{W}f''(1)$$

(32)

$$\tau_{zr}=\frac{\mu r\Omega^2}{W}\left[3+R\left(-\frac{3}{5}+\frac{M+6}{4}-\frac{3M+2\varepsilon^2}{6}+B_1+B_2\right)\right]$$

(33)

Result and Discussion: Insight into the physical occurrences within the flowing fluid can be obtained by a study of velocity profiles. The distributions of the normal velocity (w), the radial velocity (u) and azimuthal velocity (v) are plotted as a function of eta (η). Also, the pressure and shear stress variation are represented graphically.

In figure 1, 2 and 3, the radial velocity profile is plotted against η for different values of suction velocity (W) (or angular speed of the porous rotating disk (Ω)), the radius of disk (r) and Reynolds number (R) respectively. In this case, rotation of porous disk is constant, it is observed that the radial velocity profile remains negative throughout the region between the fixed impermeable disk and porous rotating disk and value becomes zero at the both disks. It decreases exponentially with increasing η from the fixed impermeable disk, reaches its minimum value and increases towards the porous rotating disk. It is also concluded that the radial velocity profile decreases with increasing the suction velocity (W) and the radius of the disk (r) in figure 1 and 2 respectively, where as, in figure 3, an increasing in Reynolds number causes increase in the radial velocity.

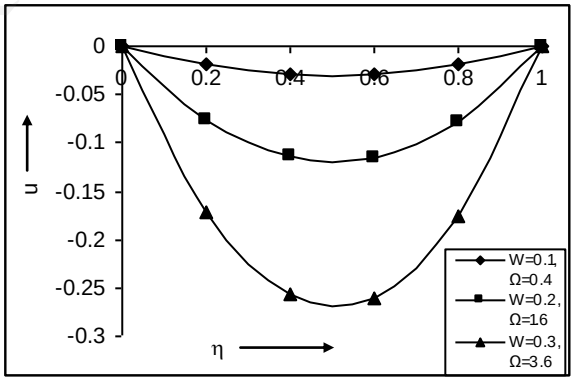

Fig.1. Radial velocity for various values of suction velocity (W) & angular speed of disk (Ω)

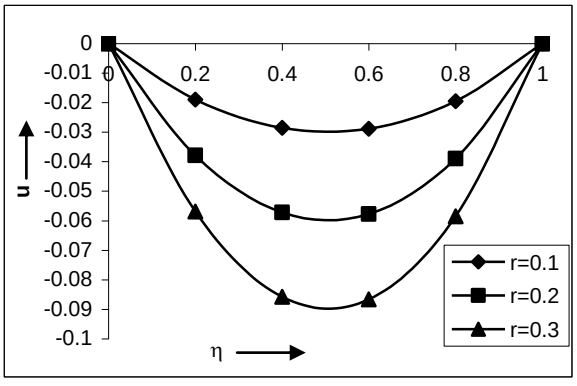

Fig.2. Radial velocity for various values of radius of disk (r)

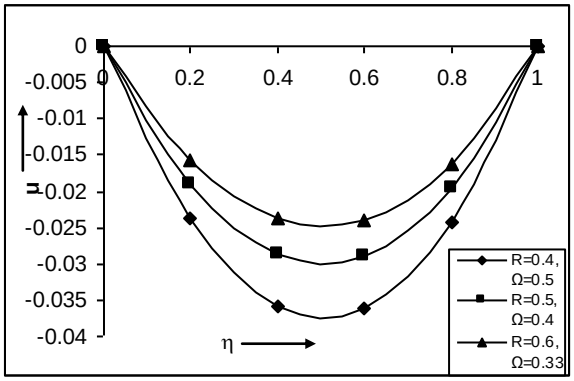

Fig.3. Radial velocity for various values of Reynolds number (R) & angular speed of disk (Ω)

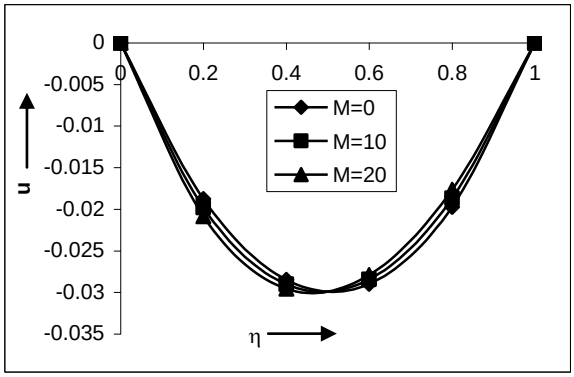

Fig.4. Radial velocity for various values of magnetic parameter (M)

Figure 4 and 5, represent the radial velocity profile for different values of the magnetic parameter (M) and the rotation of the porous disk (ε) respectively. It is observed that in both figures 4 and 5, the radial velocity profile decreases in the region $0 \leq \eta \leq 0.5$ with increasing M and ε and after that it increases towards the porous rotating disk.

In figure 6, 7, and 8, the azimuthal velocity profile (v) is plotted against η for different values of the suction parameter (W), the radius of the disk (r), and the rotation of the porous disk (ε) respectively. It is observed that the azimuthal velocity profile

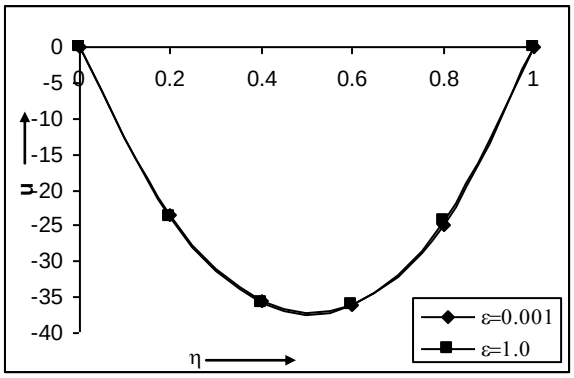

Fig.5. Radial velocity for various values of rotation of the disk (ε)

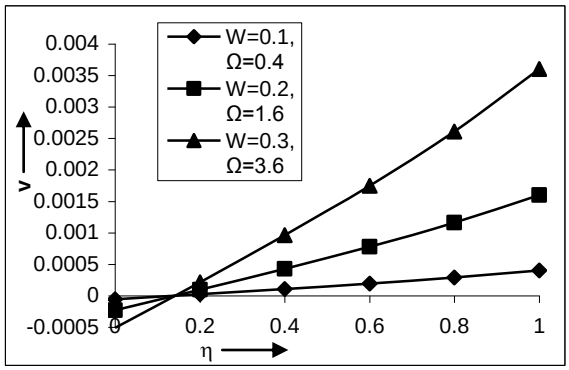

Fig.6. Azimuthal velocity for various values of suction velocity (W) & angular speed of disk (Ω)

increases continuously with increasing η towards the porous rotating disk. In fig. 6 and 7, it decreases with increasing suction velocity and the radius of the disk respectively in the region $0 \leq \eta \leq 0.14$ and after that it increases. Similarly in figure 8, the azimuthal velocity profile decreases with increasing the rotation of the porous disk in the region $0 \leq \eta \leq 0.28$ and then it increases.

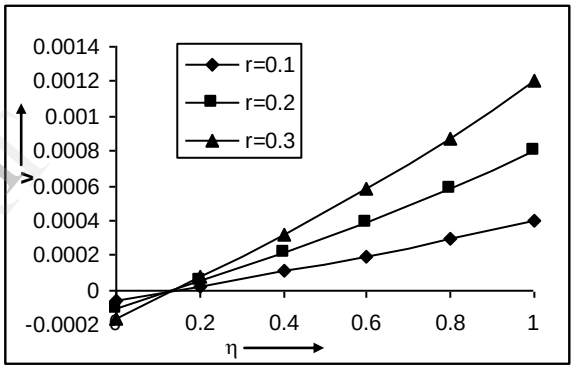

Fig.7. Azimuthal velocity for various values of radius of the disk (r)

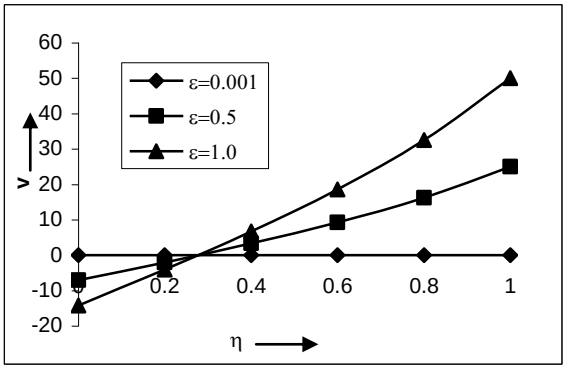

Fig.8. Azimuthal velocity for various values of rotation of the disk (ε)

Figure 9, represents the azimuthal velocity profile against η for different values of Reynolds number. It is observed that an increase in Reynolds number causes a decrease in the azimuthal velocity profile.

In figure 10, the azimuthal velocity is plotted against η for different values of the magnetic parameter (M). The azimuthal velocity increases continuously with increasing η and reaches its maximum value at the porous rotating disk (η = 1). The value of v remains positive for

M=0 and for M>0, the value of v remains negative at the fixed impermeable disk and tends to positive value towards the porous rotating disk. It is also concluded that an increase in M results a decrease in v.

Figure 11, shows the normal velocity profile (w) against η for different values of suction velocity (or angular speed of the porous rotating disk (Ω)). It is seen that the normal velocity profile increases with increasing η and reaches maximum value at the porous rotating disk. It is also observed that an increase in the suction velocity results increase in the normal velocity profile.

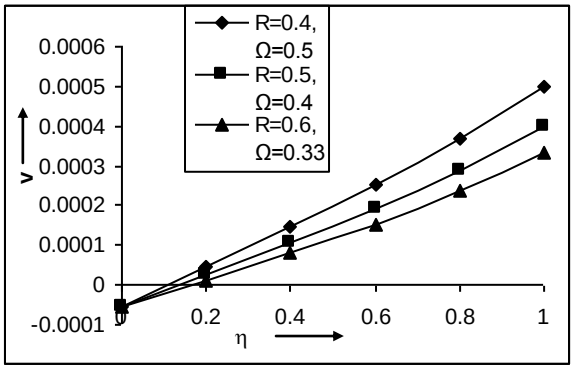

Fig.9. Azimuthal velocity for various values of Reynolds number (R) & angular speed of disk (Ω)

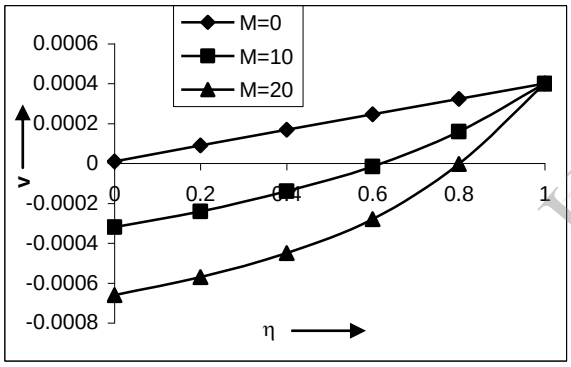

Fig.10. Azimuthal velocity for various values of magnetic parameter (M)

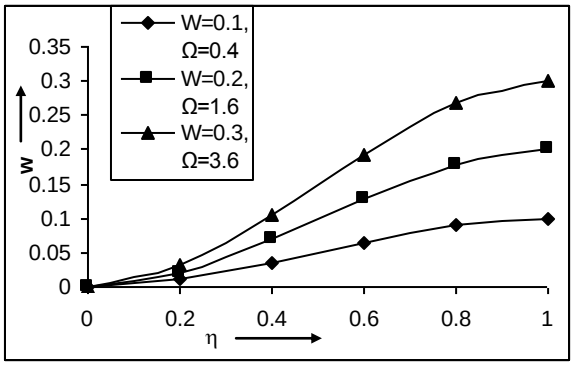

Fig.11. Normal velocity for various values of suction velocity (W) & angular speed of disk (Ω)

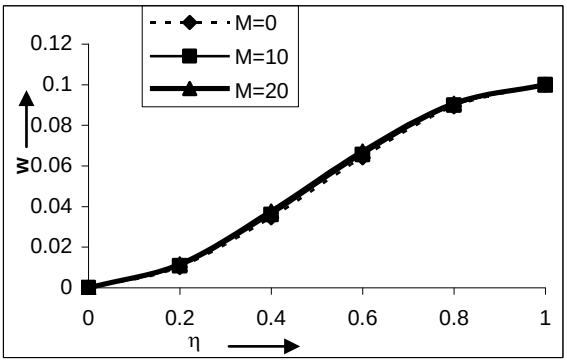

Fig.12. Normal velocity for various values of magnetic parameter (M)

In fig. 12 and 13, the normal velocity profile is plotted against η for different values of the magnetic parameter and the rotation of the porous disk. In the both figures, the normal velocity profile increases continuously with increasing η. The normal velocity profile increases with increasing the magnetic parameter and the rotation of the porous disk respectively.

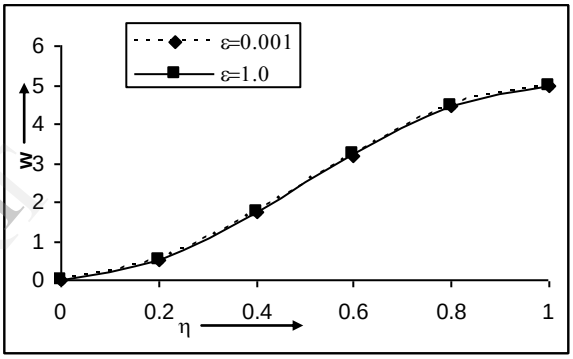

Fig.13. Normal velocity for various values of rotation of the disk (ε)

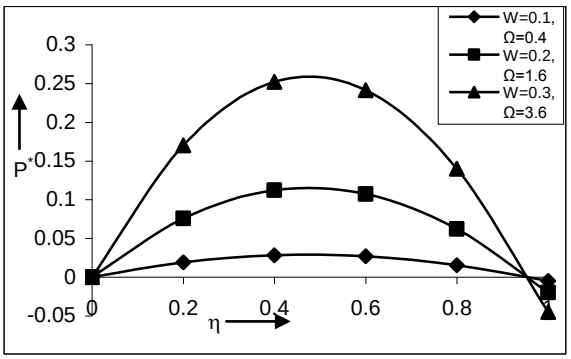

Fig.14. Fluid pressure distribution for various values of suction velocity (W) & angular speed of disk (Ω)

Figure 14 and 15, show that the fluid pressure distribution (P^*) is plotted against η for different values of the suction velocity and the Reynolds number respectively. In both figures, the fluid pressure distribution increases rapidly from the fixed impermeable disk with increasing η and reaches its maximum value and falls down towards the porous rotating disk. In figure 14, the fluid pressure distribution increases in the region $0 \leq \eta \leq 0.96$ with increasing the suction velocity and after that the fluid pressure distribution decreases towards the porous rotating disk, whereas, in figure 15, the fluid pressure distribution

decreases through out the region with increasing the Reynolds number.

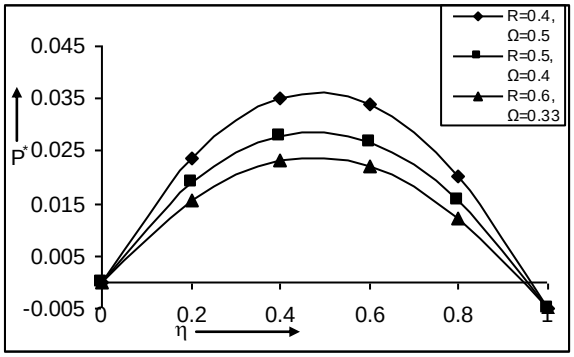

Fig.15. Fluid pressure dist. for various values of Reynolds number (R) & angular speed of disk (Ω)

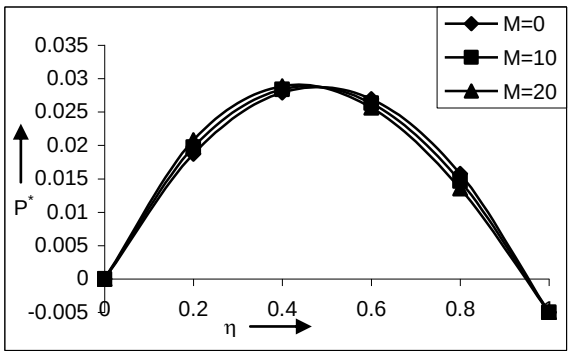

Fig.16. Fluid pressure dist. for various values of magnetic parameter (M)

In figure 16 and 17, the fluid pressure distribution is plotted against η for different values of the magnetic parameter and the rotation of the porous disk respectively. In both figures, it increases sharply with increasing η, reaches its maximum value and falls down rapidly towards the porous rotating disk. It is also observed that the fluid pressure distribution increases from the fixed impermeable disk with increasing the magnetic parameter and the rotation of the porous disk respectively in both figures, but after η > 0.48, the fluid pressure distribution decreases towards the porous rotating disk in both figures.

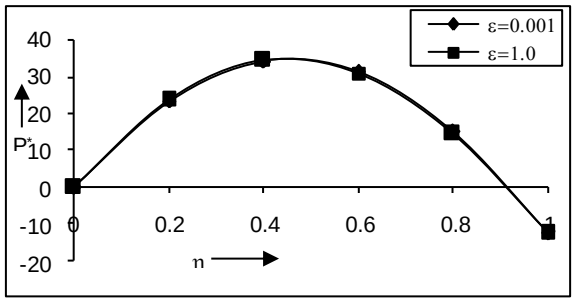

Fig.17. Fluid pressure dist. for various values of rotation of the disk (ε)

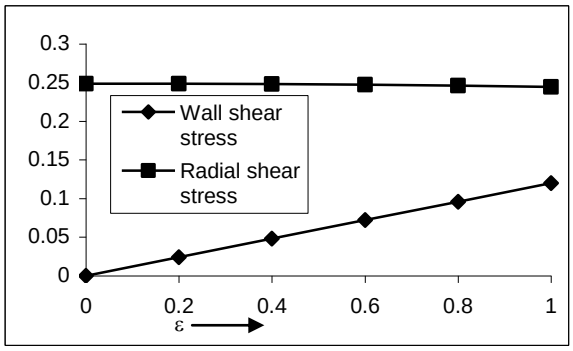

Fig.18. Effects of rotation of the disk (ε) on Wall and Radial shear stress

Figure 18 and 19, show the effects of ε and M on the wall shear stress and the radial shear stress respectively. In both figures, the wall shear stress increases steadily and the radial shear stress decreases slightly as increasing ε and M.

Figure 20 and 21, show the effects of R and W on the wall shear stress and the radial shear stress respectively. In figure 20, the wall shear stress decreases slightly and the radial shear stress decreases sharply at R=0.2 and after this , it decreases slightly as increasing R, whereas, in figure 21, both the wall shear stress and the radial shear stress increase exponentially as increasing W.

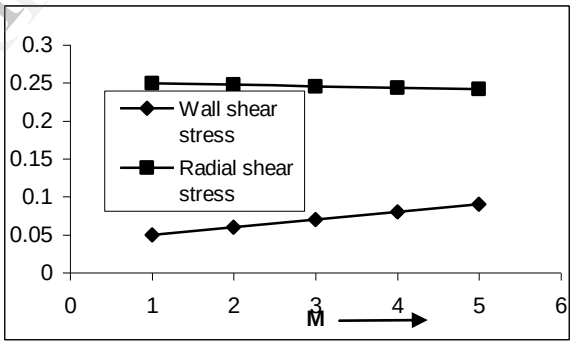

Fig.19. Effects of magnetic parameter (M) on Wall and Radial shear stress

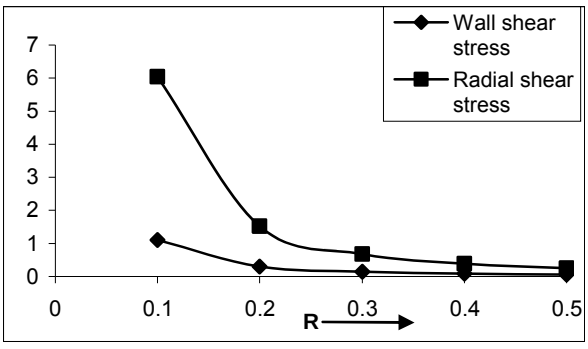

Fig.20. Effects of Reynolds number (R) on Wall and Radial shear stress

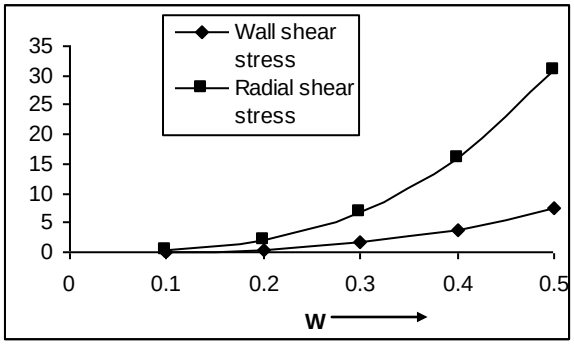

Fig.21. Effects of suction velocity (W) on Wall and Radial shear stress

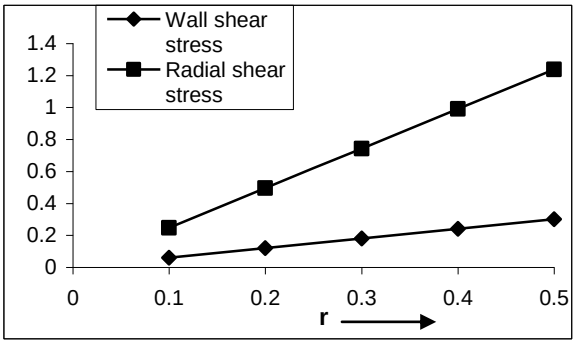

Fig.22. Effects of radius of the disk (r) on Wall and Radial shear stress

Figure 22, shows the effects of r on the wall shear stress and the radial shear stress. The wall shear stress increases slowly and the radial shear stress increases sharply as increasing r.

CONCLUSIONS:

The presence of fluid in flow between the two disks guarantees the absence of cooling and in general, cooling is felt outside the region and in front of the porous rotating disk due to suction and fluid out flow. This effect can easily be observed from a ceiling fan operation and other fan systems used in our homes.

This study presents a mathematical model in which the electrically conducting fluid is flowing between the fixed impermeable disk and the porous rotating disk in the presence of transverse magnetic field. The main findings can be summarized as:

1. The radial velocity profile decreases with increasing W and r, whereas, it increases with increasing R.
2. In positive sense, the azimuthal velocity profile increases and in negative sense, v decreases with increasing W, r and ε, whereas, it decreases as increases in R and M.
3. Increasing W, M and ε leads to an increase in the normal velocity profile.
4. An increase in W and R causes an increase in the fluid pressure distribution for W and a decrease for R.
5. The wall shear stress increases as the increasing W, M, ε and r, whereas, it decreases as the increasing R.
6. Increasing ε, M and R decreases the radial shear stress and increasing W and r increases rapidly the radial shear stress.

REFERENCES

[1] H. A. Attia, A. L. Abul-Hassan, "On hydromagnetic flow due to a rotating disk," Appl. Math. Modelling, vol. 28, pp. 1007-1014, 2004.
[2] H. A. Attia, "Unsteady flow and heat transfer of viscous incompressible fluid with temperature-dependent viscosity due to a rotating disk in a porous medium," J. Phys. A: Math. Gen., vol. 39, pp. 979-991, 2006.
[3] R. N. Barik, G. C. Dash and P. K. Rath, "Hall effects on unsteady MHD flow between two rotating disks with non-coincident parallel axes," Natl. Acad. Sci., India, Sect. A Phys. Sci., vol. 83, pp. 21-27, 2013.
[4] U. N. Das, A. Aziz, "Hydromagnetic steady flow and heat transfer of an electrically conducting viscous fluid between two rotating porous disks of different transpiration," Bull. Cal. Math. Soc., vol. 6, pp. 113-136, 1998.
[5] B. K. Das, M. Guria, R. N. Jana, "Unsteady couette flow in a rotating system," Meccanica, vol. 43, pp. 517-521, 2008.
[6] R. Ganapathy, "A note on oscillatory couette flow in a rotating system," Trans. ASME J. Appl. Mech., vol. 61, pp. 208-209, 1994.
[7] Y. N. Gaur, "Viscous incompressible flow between two infinite porous rotating disks," Indian J. Pure Appl. Math., vol. 4, p. 1289, 1972.
[8] R. N. Jana, N. Dutta, "Couette flow and heat transfer in a rotating system," Acta Mech., vol. 26, pp. 301-306, 1997.
[9] D. P. Kavenuke, E. Massawe, O. D. Makinde, "Modeling laminar flow between a fixed impermeable disk and a porous rotating disk," AJMCSR, vol. 2, pp. 157-162, 2009.
[10] N. Kelson, A. Desseasux, "Note on porous rotating flow," ANZIAM J., vol. 42, pp. 837-855, 2000.
[11] S. Khare, "Steady flow between a rotating and a porous stationary disk in presence of transverse magnetic field," Indian J. Pure Appl. Math., vol. 8, p. 808, 1977.
[12] H. K. Kuiken, "The effect of normal blowing on the flow near a rotating disk of infinite extent," J. Fluid Mech., vol. 471, pp. 789-798, 1971.
[13] G. N. Lance, M. H. Rogers, "The axially symmetric flow of a viscous fluid between two infinite rotating disks," Proc. Soc. London A, vol. 266, p. 109, 1962.
[14] A. K. Maleque, A. M. Sattar, "Steady laminar convective flow with variable properties due to a porous rotating disk," J. Heat Transfer, vol. 127, pp. 1406-1409, 2005.
[15] B. S. Mazumder, "An exact solution of oscillatory couette flow in a rotating system," Trans. ASME J. Appl. Mech., vol. 56, pp. 1104-1107, 1991.
[16] G. L. Mellor, P. J. Chappel, V. K. Stokes, "On the flow between a rotating and a stationary disk," J. Fluid Mech., vol. 31, pp. 95-112, 1968.
[17] A. K. Osalusi, P. Sibanda, "On variable laminar convective flow properties due to a porous rotating in a magnetic field," Romanian J. of Phys., vol. 51, pp. 933-944, 2006.
[18] E. Osalusi, "Effects of thermal radiation on MHD and slip flow over a porous rotating disk with variable properties," Rom. J. Phys., vol. 52, pp. 217-229, 2007.
[19] C. E. Pearson, "Numerical solutions for the time dependent viscous flow between two rotating co-axial disks," J. Fluid Mech., vol. 21, p. 613, 1965.
[20] P. Puri, "Fluctuating flow of a viscous fluid on a porous plate in a rotating medium," Acta Mech., vol. 21, pp. 153-158, 1975.
[21] G. N. Purohit, R. P. Patidar, "Steady and flow and heat transfer between two rotating disks of different transpiration," Indian J. Math., vol. 34, p. 189, 1992.
[22] P. Sibanda, O.D. Makinde, "On steady MHD flow and heat transfer past a rotating disk in a porous medium with ohmic heating and viscous dissipation.," Int. J. Numer. Methods Heat Fluid Flow, vol. 20, pp. 269–285, 2010.
[23] J. T. Stuart, "On the effect of uniform suction on the steady flow due to a rotating disk," Q. J. Mech. Appl. Math., vol. 7, pp. 446-457, 1954.
[24] M. Turkyilmazoglu, "The MHD boundary layer flow due to a rough rotating disk," ZAMM Z. Angew. Math. Mech., vol. 90, pp. 72–82, 2010.
[25] M. Turkyilmazoglu, "Exact solutions for the incompressible viscous magnetohydrodynamic fluid of a rotating disk flow," Meccanica, vol. 46, pp. 1085-1092, 2011.
[26] V. Vidyanidhi, S. D. NIgam, "Secondary flow in a rotating channel," J. Math. Phys. Sci., vol. 1, pp.35-48, 1967.